J|A|C|S ARTICLES

Published on Web 07/02/2010

Highly Selective and Sensitive DNA Assay Based on Electrocatalytic Oxidation of Ferrocene Bearing Zinc(II)−Cyclen Complexes with Diethylamine

Muhammad J. A. Shiddiky,[†] Angel A. J. Torriero,[†,‡] Zhanghua Zeng,[†,§] Leone Spiccia,*[,†,§] and Alan M. Bond*[,†,‡]

School of Chemistry, ARC Special Research Centre for Green Chemistry, and ARC Centre of Excellence for Electromaterials Science, Monash University, Clayton, Victoria 3800, Australia

Received March 13, 2010; E-mail: alan.bond@sci.monash.edu.au; leone.spiccia@sci.monash.edu.au

Abstract: A highly selective and sensitive electrochemical biosensor has been developed that detects DNA hybridization by employing the electrocatalytic activity of ferrocene (Fc) bearing cyclen complexes (cyclen = 1,4,7,10-tetraazacyclododecane, $Fc[Zn(cyclen)H_2O]_2(ClO_4)_4$ (**R1**), $Fc(cyclen)_2$ (**R2**), $Fc[Zn(cyclen)H_2O](ClO_4)_2$ (**R3**), and Fc(cyclen) (**R4**)). A sandwich-type approach, which involves hybridization of a target probe hybridized with the preimmobilized thiolated capture probe attached to a gold electrode, is employed to fabricate a DNA duplex layer. Electrochemical signals are generated by voltammetric interrogation of a Fc bearing Zn−cyclen complexes that selectively and quantitatively binds to the duplex layers through strong chelation between the cyclen complexes and particular nucleobases within the DNA sequence. Chelate formation between **R1** or **R3** and thymine bases leads to the perturbation of base-pair (A−T) stacking in the duplex structure, which greatly diminishes the yield of DNA-mediated charge transport and displays a marked selectivity to the presence of the target DNA sequence. Coupling the redox chemistry of the surface-bound Fc bearing Zn−cyclen complex and dimethylamine provides an electrocatalytic pathway that increases sensitivity of the assay and allows the 100 fM target DNA sequence to be detected. Excellent selectivity against even single-base sequence mismatches is achieved, and the DNA sensor is stable and reusable.

Introduction

The development of sensitive DNA biosensors is of critical importance in many aspects of biomedical research, including disease diagnosis, drug development, gene mapping, and DNA sequencing.[1] Such biosensors commonly rely on hybridization with DNA sequences providing a readout in the form of fluorescence,[2] chemiluminescence,[3] surface plasmon resonance,[4] quartz crystal microbalance,[5] or electrochemical[6] signals. Of these detection formats, electrochemical methods offer elegant ways for interfacing biorecognition and transduction events and represent a substantial driver to achieve selective and sensitive detection of DNA hybridization.[7] Moreover, electrochemical DNA biosensors are compatible with current miniaturization technologies employed to produce, for example, microchip-based DNA bioassays.[8]

In a typical electrochemical DNA biosensor scheme, hybridization of a DNA probe on a solid-phase support exploits the interactions between a target single-stranded (ss)-DNA and an immobilized complementary ss-DNA recognition element, which is often labeled with a redox molecule to produce an electrochemical signal.[1a] Therefore, transduction of the DNA recognition element is of considerable interest to achieve sensitive electrochemical DNA detection.[1,6] Much attention has been focused on sensitivity enhancement based on biobarcode,[9] hydrazine label,[10] functionalized liposome,[11] arrays of gold,[12] metal/semiconductor nanoparticle label,[13] redox-active reporter

[†] School of Chemistry.
[‡] ARC Special Research Centre for Green Chemistry.
[§] ARC Centre of Excellence for Electromaterials Science.

(1) (a) Palecek, E.; Fojta, M. *Anal. Chem.* **2001**, *73*, 75A. (b) Katz, E.; Willner, I. *Angew. Chem., Int. Ed.* **2004**, *43*, 6042. (c) Park, S.-J.; Taton, T. A.; Mirkin, C. A. *Science* **2002**, *295*, 1503. (d) Sassolas, A.; Leca-Bouvier, B. D.; Blum, L. J. *Chem. Rev.* **2008**, *108*, 109.
(2) (a) Gerion, D.; Parak, W. J.; Williams, S. C.; Zanchet, D.; Micheel, C. M.; Alivisatos, A. P. *J. Am. Chem. Soc.* **2002**, *124*, 7070. (b) Bruchez, M.; Moronne, M.; Gin, P.; Weiss, S.; Alivisatos, A. P. *Science* **1998**, *281*, 2013. (c) Chan, W. C. W.; Nie, S. M. *Science* **1998**, *281*, 2016.
(3) Miao, W.; Bard, A. J. *Anal. Chem.* **2004**, *76*, 5379.
(4) (a) He, L.; Musick, M. D.; Nicewarner, S. R.; Salinas, F. G.; Benkovic, S. J.; Natan, M. J.; Keating, C. D. *J. Am. Chem. Soc.* **2000**, *122*, 9071. (b) Fang, S.; Lee, H. J.; Wark, A. W.; Corn, R. M. *J. Am. Chem. Soc.* **2006**, *128*, 14044.
(5) Yao, C.; Zhu, T.; Tang, J.; Wu, R.; Chen, Q.; Chen, M.; Zhang, B.; Huang, J.; Fu, W. *Biosens. Bioelectron.* **2008**, *23*, 879.
(6) Drummond, T. G.; Hill, M. G.; Barton, J. K. *Nat. Biotechnol.* **2003**, *21*, 1192.
(7) (a) Kuhr, W. G. *Nat. Biotechnol.* **2000**, *18*, 1042. (b) Willner, I. *Science* **2002**, *298*, 2407.
(8) (a) Liu, D.; Perdue, R. K.; Sun, L.; Crooks, R. M. *Langmuir* **2004**, *20*, 5905. (b) Khandurina, J.; Jacobson, S. C.; Waters, L. C.; Foote, R. S.; Ramsey, J. M. *Anal. Chem.* **1999**, *71*, 1815. (c) Shiddiky, M. J. A.; Shim, Y. -B. *Anal. Chem.* **2007**, *79*, 3724.
(9) (a) Stoeva, S. K.; Lee, J. -S.; Thaxton, C. S.; Mirkin, C. A. *Angew. Chem., Int. Ed.* **2006**, *45*, 3303. (b) He, P.; Shen, L.; Cao, Y.; Li, D. *Anal. Chem.* **2007**, *79*, 8024.
(10) (a) Shiddiky, M. J. A.; Rahman, M. A.; Shim, Y. -B. *Anal. Chem.* **2007**, *79*, 6886. (b) Shiddiky, M. J. A.; Rahman, M. A.; Cheol, C. S.; Shim, Y.-B. *Anal. Biochem.* **2008**, *379*, 170.
(11) Patolsky, F.; Lichtenstein, A.; Willner, I. *Angew. Chem., Int. Ed.* **2000**, *39*, 940.

molecule and enzyme label,[14] redox marker-, gold-, and enzyme-loaded microsphere,[15] aptamer,[16] and enzyme−carbon nanotube architectures.[17] While these methods generally have very low detection limits (even lower than 1.0 fM), their practical application is restricted due to the complicated detection procedures (e.g., multiple redox cycling) or conjugation chemistries (e.g., labeling of enzymes and nanoparticles, etc.). Thus, it is still a major challenge to develop new technologies with improved simplicity, selectivity, and sensitivity of DNA hybridization detection that do not require complicated fabrication, instrumentation, and additional reagents.

Barton and co-workers[18,19] have developed an electrochemical method that can detect single-base mismatches without requiring complicated fabrication and stringent washings. The method combines redox active intercalators to achieve charge transport through the base-pair stacking of DNA duplexes. Duplex-modified electrodes exhibit high affinities for DNA-binding substrates and promote efficient electron transfer between the electrodes and duplex-bound intercalators. Any perturbation of the base-pair stacking (e.g., mismatched base pairing) greatly decreases the efficiency of charge transfer through the duplex with a concomitant diminution in electrochemical current and hence enables mismatches to be detected.[18,19] This concept of using charge transport has been extended by Gooding and co-workers for electrochemical monitoring of DNA−drug interaction based on a reduction in DNA-mediated charge transport upon drug binding and thereby shutting off the electrochemical signal.[20] In this study, we exploit a new strategy for monitoring electrochemical DNA hybridization based on the charge transport through the ferrocene (Fc) bearing Zn(II)−cyclen complex-bonded duplex DNA layers.

Cyclen complexes bearing a ferrocene (Fc) moiety ($Fc[Zn(cyclen)H_2O]_2(ClO_4)_4$ (**R1**)[21] and $Fc[Zn(cyclen)H_2O](ClO_4)_2$ (**R3**),[22] cyclen = 1,4,7,10-tetraazacyclododecane) can bind to the DNA sequence at specific positions. In particular, Zn(II)−cyclen has been shown to selectively bind strongly to an imide-containing nucleobase, deoxythymidine (dT), in aqueous solution (dissociation constant, $K_d = [\text{free dT}][\text{free Zn(II)−cyclen}]/[dT^- - Zn(II) - \text{cyclen}] = 8 \times 10^{-4}$ M at pH 7.4[23a]). The binding between the Zn(II)−cyclen and dT-rich region dissociates A−T hydrogen bonds and changes the local conformation in the double-stranded (ds)-DNA.[23d−f] In addition, through the incorporation of redox active ferrocenyl units, these molecules can be used as labels for direct electrochemical recognition of DNA sequence to produce a highly biocompatible electrochemical DNA biosensor. An electrochemical DNA sensor employing a Fc bearing naphthalene derivative has been developed,[23g] in which the voltammetric signal achieved is due to the redox reaction of the Fc moiety bound to the surface-attached ds-DNA. Previously, we[21,22] and others[23a] have illustrated that the Zn(II)−cyclen and bis(Zn(II)−cyclen) complexes offer remarkable selectivity in the recognition of the thymidine neucleotide and thymidilyl(3−5)thymidine (TpT) under physiological conditions. More recently, we have synthesized and characterized a TpT receptor that contains two Zn(II)−cyclen complexes bridged by a ferrocenyl moiety (**R1**).[22] The distance between the two cyclopentadienyl rings in ferrocene (3.3 Å) is almost equivalent to that separating two stacked pairs in DNA sequences. Consequently, **R1** forms a stable adduct (apparent binding constant, $K_{app} = 0.89 \pm 0.10 \times 10^6$ M^{-1}) with TpT, and its complexation with the TpT groups could be monitored electrochemically.[22]

It is well-known that electrocatalytic schemes can be used to enhance the current derived from electroactive species.[19] In an electrocatalytic scheme, an excess of substrate that acts as reducing or oxidizing agents is required to regenerate a starting electroactive species.[24a] This approach has been developed for the electrocatalytic detection of DNA hybridization based on labeling of the surface-attached duplex DNA with Fc-labels, where the electrocatalysis relies on the electrochemical signal originating from the electron transfer between the substrate in solution and the electrode mediated by the redox centers on the duplex DNA.[25] To enhance the charge transduction through duplex DNA, Barton and co-workers coupled the DNA-mediated charge transport to an electrocatalytic reaction by adding the freely diffusing ferricyanide to the electrolyte solution.[19]

Here, we report the electrochemical detection of DNA hybridization using the Fc bearing cyclen complex covalently bound to DNA duplex layers on a gold electrode. The binding

(12) Patolsky, F.; Ranjit, K. T.; Lichtenstein, A.; Willner, I. *Chem. Commun.* **2000**, 1025.

(13) (a) Wang, J.; Xu, D.; Kawde, A. N.; Polsky, R. *Anal. Chem.* **2001**, *73*, 5576. (b) Hansen, J. A.; Mukhopadhyay, R.; Hansen, J. O.; Gothelf, K. V. *J. Am. Chem. Soc.* **2006**, *128*, 3860. (c) Liu, G.; Lin, Y. *J. Am. Chem. Soc.* **2007**, *129*, 10394. (d) Willner, I.; Patolsky, F.; Wasserman, J. *Angew. Chem., Int. Ed.* **2001**, *40*, 1861. (e) Selvaraju, T.; Das, J.; Jo, K.; Kwon, K.; Huh, C. -H.; Kim, T. K.; Yang, H. *Langmuir* **2008**, *24*, 9883.

(14) (a) Palecek, E.; Fojta, M.; Jelen, F. *Bioelectrochemistry* **2002**, *56*, 85. (b) Yang, I. V.; Thorp, H. H. *Anal. Chem.* **2001**, *73*, 5316. (c) Floch, F. L.; Ho, H.-A.; Lepage, P. H.; Bedard, M.; Neagu-Plesu, R.; Leclerc, M. *Adv. Mater.* **2005**, *17*, 1251. (d) Luo, X.; Lee, T. M.-H.; Hsing, I. -M. *Anal. Chem.* **2008**, *80*, 7341. (e) Xiao, Y.; Lubin, A. A.; Baker, B. R.; Plaxco, K. W.; Heeger, A. J. *Proc. Natl. Acad. Sci. U.S.A.* **2006**, *103*, 16677. (f) Zhang, Y.; Pothukuchy, A.; Shin, W.; Kim., Y.; Heller, A. *Anal. Chem.* **2004**, *76*, 4093. (g) Wang, J.; Liu, G.; Rasul, M. *J. Am. Chem. Soc.* **2003**, *126*, 3010.

(15) (a) Wang, J.; Polsky, R.; Merkoci, A.; Turner, K. L. *Langmuir* **2003**, *19*, 989. (b) Kawde, A.-N.; Wang, J. *Electroanalysis* **2004**, *16*, 101. (c) Wang, J.; Kawde, A.-N.; Jan, M. R. *Biosens. Bioelectron.* **2004**, *20*, 995.

(16) Zayats, M.; Huang, Y.; Gill, R.; Ma, C.; Willner, I. *J. Am. Chem. Soc.* **2006**, *128*, 12668.

(17) Munge, B.; Liu, G.; Collins, G.; Wang, J. *Anal. Chem.* **2005**, *77*, 4662.

(18) (a) Holmlin, R. E.; Dandliker, P. J.; Barton, J. K. *Angew. Chem., Int. Ed.* **1997**, *36*, 2714. (b) Kelly, S. O.; Barton, J. K. *Science* **1999**, *283*, 375. (c) Kelly, S. O.; Jackson, N. M.; Hill, M. G.; Barton, J. K. *Angew. Chem., Int. Ed.* **1999**, *38*, 941. (d) Kelly, S. O.; Boon, E. M.; Barton, J. K.; Jackson, N. M.; Hill, M. G. *Nucleic Acids Res.* **1999**, *27*, 4830.

(19) (a) Boon, E. M.; Cered, D. M.; Drummond, T. G.; Hill, M. G.; Barton, J. K. *Nat. Biotechnol.* **2000**, *18*, 1096. (b) Kelly, S. O.; Barton, J. K. *Bioconjugate Chem.* **1997**, *8*, 31. (c) Genereux, J. C.; Barton, J. K. *Chem. Rev.* **2010**, *110*, 1642.

(20) (a) Gooding, J. J. *Electroanalysis* **2002**, *14*, 1149. (b) Wong, E. L. S.; Erohkin, P.; Gooding, J. J. *Electrochem. Commun.* **2004**, *6*, 648. (c) Wong, E. E. S.; Gooding, J. J. *J. Am. Chem. Soc.* **2007**, *129*, 8950. (d) Wong, E. E. S.; Gooding, J. J. *Anal. Chem.* **2006**, *78*, 2138.

(21) Gasser, G.; Belousoff, M. J.; Bond, A. M.; Kosowski, Z.; Spiccia, L. *Inorg. Chem.* **2007**, *46*, 1665.

(22) Zeng, Z.; Torriero, A. A. J.; Belousoff, M. J.; Bond, A. M.; Spiccia, L. *Chem.—Eur. J.* **2009**, *15*, 10988.

(23) (a) Shionoya, M.; Kimura, E.; Shiro, M. *J. Am. Chem. Soc.* **1993**, *115*, 6730. (b) Kikuta, E.; Murata, M.; Katsube, N.; Koike, T.; Kimura, E. *J. Am. Chem. Soc.* **1999**, *121*, 5426. (c) Aoki, S.; Kimura, E. *Chem. Rev.* **2004**, *104*, 769. (d) Kikuta, E.; Aoki, S.; Kimura, E. *J. Biol. Inorg. Chem.* **2002**, *4*, 473. (e) Kikuta, E.; Koike, T.; Kimura, E. *J. Inorg. Biochem.* **2000**, *79*, 253. (f) Kinoshita-Kikuta, E.; Kinoshita, E.; Koike, T. *Nucleic Acids Res.* **2002**, *30*, e126. (g) Takenaka, S.; Yamashita, K.; Takagi, M.; Uto, Y.; Kondo, H. *Anal. Chem.* **2000**, *72*, 1334.

(24) (a) Bard, A. J.; Faulkner, L. R. *Electrochemical Methods: Principles and Applications*, 2nd ed.; John Wiley & Sons: New York, 2001; pp 501−503. (b) Coury, L. A., Jr.; Oliver, B. N.; Egekeze, J. O.; Sosnoff, C. S.; Brumfield, J. C.; Buck, R. P.; Murray, R. W. *Anal. Chem.* **1990**, *62*, 452.

Table 1. Oligonucleotide Sequences and Modifications

name	sequence
capture probe 1 (CP1)	5′-HS$(CH_2)_6$-AAAGAAGCCAGCTCAAGCAATATTAATGAAG-3′
capture probe 2 (CP2)	5′-HS $(CH_2)_6$-CAAGCCGCCCGCGCCCGCCCGCGGCCGGCCG-3′
capture probe 3 (CP3)	5′-HS-$(CH_2)_6$-CCCGCCGCCCGCGCCCGCCCGCGGCCGGAAG-3′
capture probe 4 (CP4)	5′-HS $(CH_2)_6$-ACAGCCGCCCGCGCCCGCCCGCGGCCGGCCG-3′
capture probe 5 (CP5)	5′-HS-$(CH_2)_6$-CCCGCCGCCCGCGCCCGCCCGCGGCCGGCCG-3′
target probe 1 (TP1)	5′-CTTCATTAATATTGCTTGAGCTGGCTTCTTT-3′
noncomplementary (NC)	5′-CTTCATTAATATTGCTTGAGCGACTTAAGAT-3′
single-base mismatch (SM)	5′-CTTCATTAATATTGCTTGAGCTGGCT**C**CTTT-3′
target probe 2 (TP2)	5′-CGGCCGGCCGCGGGCGGGCGCGGGCGGC**TT**G-3′
target probe 3 (TP3)	5′- C**TT**CCGGCCGCGGGCGGGCGCGGGCGGCGGG-3′
target probe 4 (TP4)	5′-CGGCCGGCCGCGGGCGGGCGCGGGCGGC**TGT**-3′
target probe 5 (TP5)	5′- CGGCCGGCCGCGGGCGGGCGCGGGCGGCGGG-3′

Scheme 1. Schematic Representation of the Fabrication of a DNA Sensing Layer on a Gold Electrode

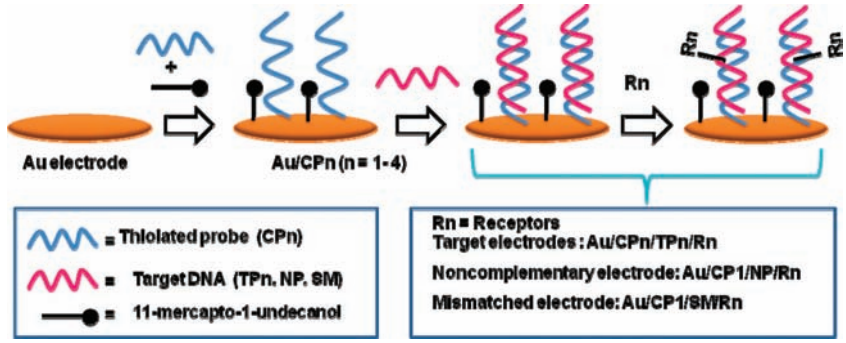

of thymine or TpT to either **R1** or **R3** causes perturbation of the A−T base-pair stacking in the DNA structure, which hinders the charge transport through the duplex layers. Experimental parameters, such as incubation time and ionic strength of the solutions, were optimized to obtain effective electrochemical responses for DNA-mediated charge transport of the $Fc^{0/+}$ process. Under optimized conditions and when coupled with an electrocatalytic cycle involving diethylamine, the response of a surface-immobilized target associated with the duplex layers effectively reports the presence of target DNA. The resulting assay exhibits greatly enhanced selectivity for discrimination between the complementary, noncomplementary, and single-base mismatched DNA sequences and allows the sensitive electrochemical detection of DNA.

Experimental Section

Materials. Chemicals were obtained from either Sigma or Aldrich and used as received, unless otherwise stated. Aqueous solutions were prepared with distilled deionized water (Milli-Q filtering system). In voltammetric studies, nitrogen gas was passed through the solutions for 20 min. A nitrogen atmosphere was then maintained above the solution during measurements. The oligonucleotides were obtained from either Genemed Synthesis, Inc. (TX, USA) or Micromon, Monash University (Vic, Aus). Table 1 lists the DNA sequences and modified oligonucleotides used in this work. The receptors, **R1**, $Fc(cyclen)_2$ (**R2**), **R3**, and Fc(cyclen) (**R4**), were synthesized following published procedures.[21,22,26]

Fabrication of Receptor-Modified DNA Sensors. The DNA sensors were fabricated on polycrystalline gold (Au) disk electrodes ($d = 1.6$ mm; BAS, West Lafayette, IN) (Scheme 1). The electrode was mechanically polished with an alumina slurry (0.05 μm, Buehler), washed with water, and electrochemically cleaned by cycling the potential between −0.1 and 1.3 V (vs Ag/AgCl) 0.1 M H_2SO_4 until a stable voltammogram was obtained. The clean electrode was then modified with a thiolated capture probe and a diluent layer (1.0 mM ethanolic 11-mercapto-undecanol (MCU)) by immersing the clean gold electrodes in 4.0 μM solutions of capture probe (CP1, CP2, CP3, or CP4) in 100 mM phosphate buffer (1.0 M NaCl, 1.0 mM $MgCl_2$, pH 7.4) for 12 h at room temperature followed by immersion in a 1.0 mM MCU solution for 2 h, and then by rinsing with the 100 mM tris-HCl buffer solution twice (approximately for 5 s) to remove any physically adsorbed species. Prior to the immobilization of the thiolated capture probes, they were incubated for 2 h in 4.0 μM tris-(2-carboxyethyl)phosphine hydrochloride solution to reduce the disulfide-bound oligomer.[27] Hybridization with the target (TP1, TP2, TP3, or TP4), noncomplementary (NC), and single-base mismatched (SM) DNA probes was performed by immersion in appropriate concentrations of the sequence in the hybridization buffer (20 mM tris-(hydroxymethyl)aminomethane hydrochloride (tris), 200 mM NaCl, and 0.5% Tween 20 (pH 7.4)) for 4 h (hereafter referred to as Au/CP1/TP1-, Au/CP2/TP2-, Au/CP3/TP3-, Au/CP4/TP4-, Au/CP1/NC-, and Au/CP1/SM-modified electrodes).

The duplex-modified sensing layers were immersed in a buffer (100 mM tris-HCl buffer, pH 7.4) solution containing a particular concentration of the receptor for a designated time to obtain receptor-functionalized modified electrodes. The electrodes were rinsed with the 100 mM tris-HCl buffer solution twice (approximately for 5 s) to remove nonspecifically adsorbed receptor molecules and dried under nitrogen gas.

Electrochemical Measurements. Experiments employing cyclic voltammetry (CV), Osteryoung square-wave voltammetry (OSWV), and chronocoulometry were conducted at 21 ± 1 °C in a standard three-electrode electrochemical cell arrangement using a BAS model 100B electrochemical workstation (Bioanalytical Systems, West

(25) (a) Mir, M.; Álvarez, M.; Azzaroni, O.; Tiefenauer, L.; Knoll, W. *Anal. Chem.* **2008**, *80*, 6554. (b) Azzaroni, O.; Álvarez, M.; Mir, M.; Yameen, B.; Knoll, W. *J. Phys. Chem. C* **2008**, *112*, 15850. (c) Patolsky, F.; Weizmann, Y.; Willner, I. *J. Am. Chem. Soc.* **2002**, *124*, 770.

(26) Boldrini, V.; Giovenzana, G. B.; Pagliarin, R.; Pamisano, G.; Sisti, M. *Tetrahedron Lett.* **2000**, *41*, 6527.

(27) Xiao, Y.; Lai, R. Y.; Plaxco, K. W. *Nat. Protoc.* **2007**, *2*, 2875.

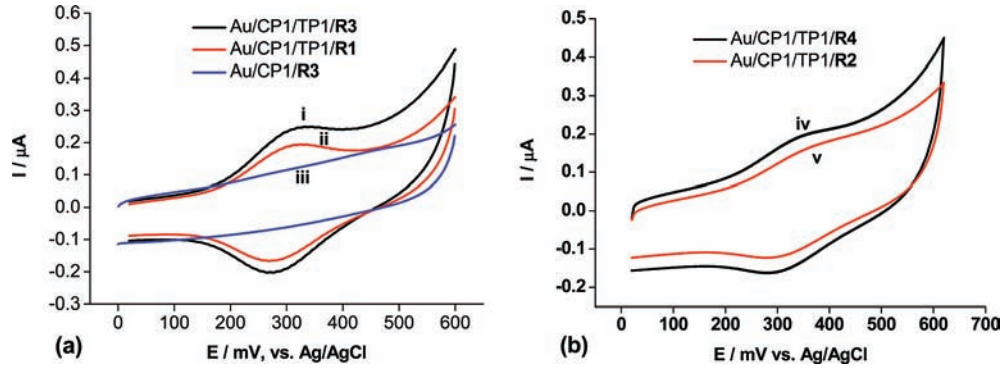

Figure 1. Cyclic voltammograms obtained at a scan rate of 100 mV s^{-1} at (a) **R1**- and **R3**-functionalized and (b) **R2**- and **R4**-functionalized electrodes when 160 nM TP1 was hybridized to the thiolated ss-DNA probe in a 100 mM tris-HCl (pH 7.4) buffer solution.

Lafayette, IN, USA). The electrochemical cell consisted of the DNA sensor working electrode, a platinum wire counter electrode, and a Ag/AgCl (3.0 M NaCl) reference electrode. The background electrolyte was 100 mM tris-HCl (pH 7.4) buffer solution. The electrocatalytic currents at duplex sensing layers were measured by cyclic voltammetry in background electrolyte containing 2.5 mM diethylamine.

Surface Density of DNA. The surface density of DNA sequences (1.86×10^{12} molecules cm^{-2}) was determined by the chronocoulometric method as described by Tarlov et al.[28] and Gooding et al.[20c] The chronocoulometric plots (charge vs square root of time, see Figure S1 in Supporting Information) of the DNA recognition surface for the 5.0 nM TP1 probe was obtained in 10 mM tris-HCl (pH 7.4) buffer. The cationic redox active ruthenium(III) hexaammine ($[Ru(NH_3)_6]^{3+}$) (50 μM) was then introduced into the buffer solution and allowed to equilibrate for 1 min followed by chronocoulometric measurement. The surface coverage of $[Ru(NH_3)_6]^{3+}$ was calculated as the difference in the chronocoulometric intercepts in the absence and presence of $[Ru(NH_3)_6]^{3+}$ and converted to the DNA surface density using the relationship $\Gamma_{DNA} = \Gamma_0(z/m)$, where Γ_{DNA} = surface density of the DNA, Γ_0 = surface coverage of $[Ru(NH_3)_6]^{3+}$, z = charge of the $[Ru(NH_3)_6]^{3+}$, and m = the number of DNA bases.[28,20c]

Results and Discussion

Cyclic Voltammetry of the Receptor-Functionalized Electrodes. Figures 1a and b display cyclic voltammetric features for the detection of 160 nM TP1 sequences at the Au/CP1/TP1/**R3** (i), Au/CP1/TP1/**R1** (ii), Au/CP1/TP1/**R4** (iv), and Au/CP1/TP1/**R2** (v) electrodes in 100 mM tris-HCl buffer solution. At pH 7.4, all four electrodes exhibited well-defined surface-bound redox chemistry associated with the $Fc^{0/+}$ process.[24] In contrast, no Faradaic current response was observed under conditions of cyclic voltammetry at the control electrode (Figure 1a (iii)), although some was detectable when the more sensitive square-wave voltammetric technique was employed (see below). The oxidation peak current at all electrodes linearly increases with the scan rate up to 1000 mV s^{-1}. The peak-to-peak separation (ΔE_p) between the oxidative peak potential, E_p^{ox}, and reductive peak potential, E_p^{red}, at these electrodes is 38 $\pm$ 5 mV vs Ag/AgCl at a scan rate of 100 mV s^{-1}. The midpoint potential (E_m) for the surface-bound $Fc^{0/+}$ process, calculated from the average of E_p^{ox} and E_p^{red} values found at the Au/CP1/TP1/**R1**, Au/CP1/TP1/**R3**, Au/CP1/TP1/**R2**, and Au/CP1/TP1/**R4** electrodes are 300 $\pm$ 5, 300 $\pm$ 5, 320 $\pm$ 5, and 320 $\pm$ 5 mV vs Ag/AgCl, respectively. In comparison, E_m at a bare Au electrode is 340 $\pm$ 3 mV vs Ag/AgCl. Thus, a 40 $\pm$ 5 mV negative shift in the E_m values for the surface-bound $Fc^{0/+}$ process is observed at the Au/CP1/TP1/**R1** and Au/CP1/TP1/**R3** electrodes. The negative shift in E_m for the Au/CP1/TP1/**R2** and Au/CP1/TP1/**R4** electrodes was 20 $\pm$ 5 mV. An analogous voltammetric characteristic was reported for TpT binding to **R1**.[22] These data indicate that **R1**, **R2**, **R3**, and **R4** have an affinity for nucleobases and nucleotides present in the DNA duplex structure which should allow the electrochemical detection of DNA hybridization using the DNA-mediated charge transport of the surface-bound $Fc^{0/+}$ process.

Binding Mechanism and Optimization of the Binding Conditions. As seen in Figure 1, the voltammetric behavior of the receptor-functionalized electrodes is markedly influenced by the binding of the receptors **R*n*** (n = 1−4) with the nucleobases and nucleotides in the DNA sequences. Scheme 2 shows the binding mechanism of **R1** and **R3** with the duplex DNA layer. Our hypothesis is that **R1** interaction with the imide groups of TpT (Scheme 2A) or thymine (Scheme 2B) requires the deprotonation of Zn(II) followed by the formation of a Zn(II)−imide covalent bond. It is well established that the two carbonyls adjacent to the imide enhance complexation by forming hydrogen bonds with the NH hydrogens, which occupy the 4- and 10-positions of the cyclen molecule. As a consequence, *two* three-point interactions of **R1** with the DNA-duplex structure can occur. In contrast, complex formation between **R3** and the CP1/TP1 duplex structure involves only *one* three-point binding interaction (Scheme 2C). For **R1**, the two three-point bindings on the TpT units in the TP1 sequence force the two positively charged *trans*-(Zn(II)−cyclen) units to rearrange in a *cis* configuration, in the manner previously proposed for chelate formation between **R1** and TpT.[22] These binding interactions disrupt the hydrogen bonds of A−T base pairs in duplex DNA layers and perturb the base-pair stacking, resulting in a reduction of the duplex-mediated charge transport.

The binding efficiency of **R1** and **R3** to A−T regions in the duplex layer is largely dependent on the ionic strength of the solution and incubation time for the binding of **R1** and **R3**. Experiments to optimize these parameters used the square-wave voltammetric responses obtained when Au/CP1/TP1/**Rn** (n = 1−4)-modified electrodes are used in the presence of the TP1 target sequence. Figures 2a and 2b show the responses of the Au/CP1/TP1/**R1** and Au/CP1/TP1/**R3** electrodes obtained after incubating the Au/CP1/TP1 duplex layers with 0.25 μM solution of **R1** and **R3**, respectively, for designated incubation times. In both cases, as the incubation proceeded, the perturbation of the A−T base pair stacking in the duplex structure increased with increasing **R1** and **R3** attachment, resulting in suppression of

(28) Steel, A. B.; Herne, T. M.; Tarlov, M. J. *Anal. Chem.* **1998**, *70*, 4670.

Scheme 2. Schematic Representation of the Binding of **R1** and **R3** with Duplex DNA Layers

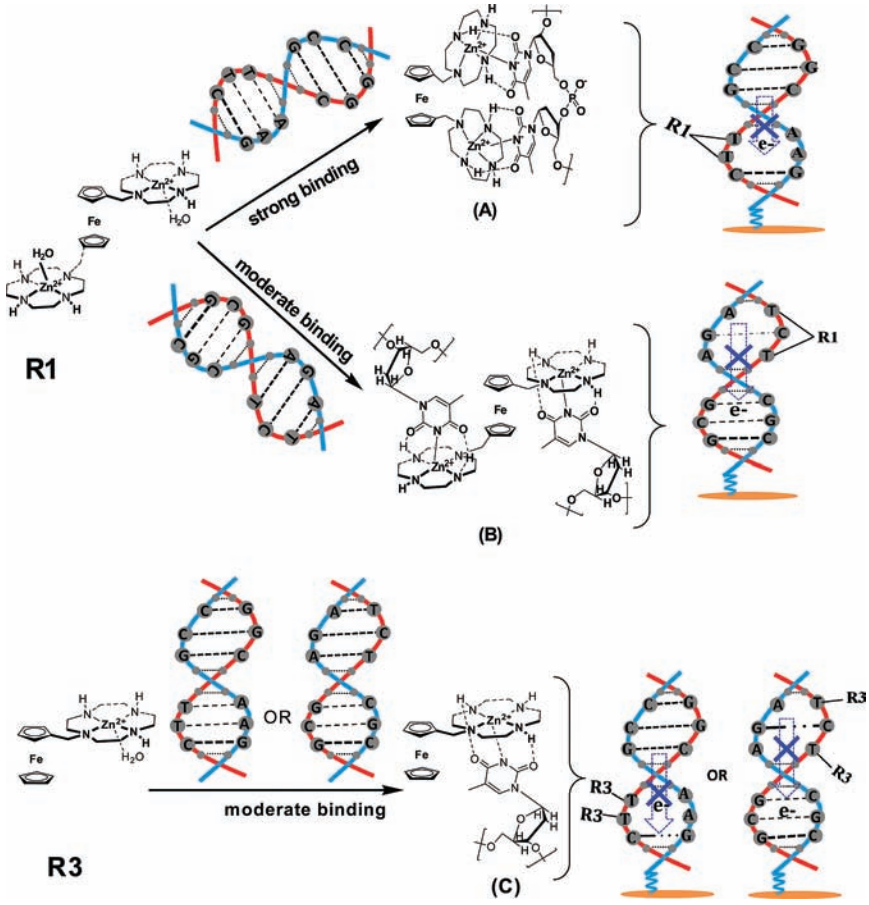

the current. These results indicate that long-range charge transport is inhibited by disruption of the base pair stacking in the DNA duplex layers, in accord with the reported diminished charge transport through a DNA duplex, upon binding of *cis*-diaminedichloroplatinum(II).[20c] The incubation times required to ensure complete attachment of the complexes, and hence complete disruption of the duplex structure, as determined by complete absence of oxidation at the Au/CP1/TP1/**R1** and Au/CP1/TP1/**R3** electrode are 8 and 12 min, respectively. Notably, measurable peak currents at both the Au/CP1/TP1/**R1** and Au/CP1/TP1/**R3** electrodes were obtained after 1 min of incubation, the time used for all further experiments conducted with **R1**- or **R3**-functionalized electrodes.

The suppression of the peak currents at the **R1**- and **R3**-functionalized electrodes contrasts with findings for the Au/CP1/TP1/**R2** and Au/CP1/TP1/**R4** electrodes (Figures S2a and S2b, Supporting Information) where the oxidation peak currents increase with incubation time. The increase is due to the interaction of **R2** and **R4** molecules with the duplex surfaces via hydrogen bonding between protonated **R2** or **R4** molecules and phosphate moieties of the duplex DNA structure occurring without perturbing the base-pair stacking (Schemes S1 and S2, Supporting Information). Note that the **R2** receptor can bind to two phosphate groups within the duplex layer, whereas **R4** can only bind to one phosphate group. For **R4**, a larger number of molecules can interact with the duplex backbone, resulting in a larger number of Fc moieties on the **R4**-functionalized electrode. Thus, the Au/CP1/TP1/**R4** electrode offers higher sensitivity than that obtained for the Au/CP1/TP1/**R2** electrode. The shorter incubation time required for the Au/CP1/TP1/**R4** electrode (15 min vs 20 min) to achieve maximum peak currents is consistent with these observations. Notably, the peak current at the 100 nM TP1-bound duplex electrode obtained after 15 min of the incubation in **R2** or **R4** solution is much lower than that obtained for a 1 min incubation of the 25 nM TP1-bound duplex electrode in **R1** or **R3** solutions.

The effect of concentration of **R1** and **R3** on the current magnitude for a 25 nM TP1 sequence modified duplex electrode is shown in Figures 2c and 2d. The peak current decreases with increasing concentration of **R1** and **R3**. At sufficiently high concentrations of **R1** or **R3**, a plateau or minimum value of the peak current was obtained. For a 1 min incubation time, the lowest concentration of **R1** and **R3** needed to attain a measurable peak current at the Au/CP1/TP1/**R1** and Au/CP1/TP1/**R3** electrodes was 0.25 μM. A higher oxidation peak current was observed at the Au/CP1/TP1/**R3** modified electrode when similar concentrations of **R1** and **R3** (0.25 μM) were used to fabricate the Au/CP1/TP1/**R1** and Au/CP1/TP1/**R3** sensing layers. This is again due to the lower disruption of the base pairs in the duplex layer and hence faster charge transport through the duplex. In contrast, the peak currents for the 100 nM target sequence increase with the concentration of **R2** and **R4** (Figures S2c and S2d, Supporting Information). The maximum peak currents at the Au/CP1/TP1/**R2** and Au/CP1/TP1/**R4** electrodes were attained after incubating the Au/CP1/TP1 duplex electrode in 2.5 μM **R2** and 2.5 μM **R4** for 20 and 15 min, respectively. From the above results, the concentrations of **R1**, **R3**, **R2**, and **R4** chosen for the determination of the target DNA on the duplex electrode were 0.25, 0.25, 2.5, and 2.5 μM, respectively.

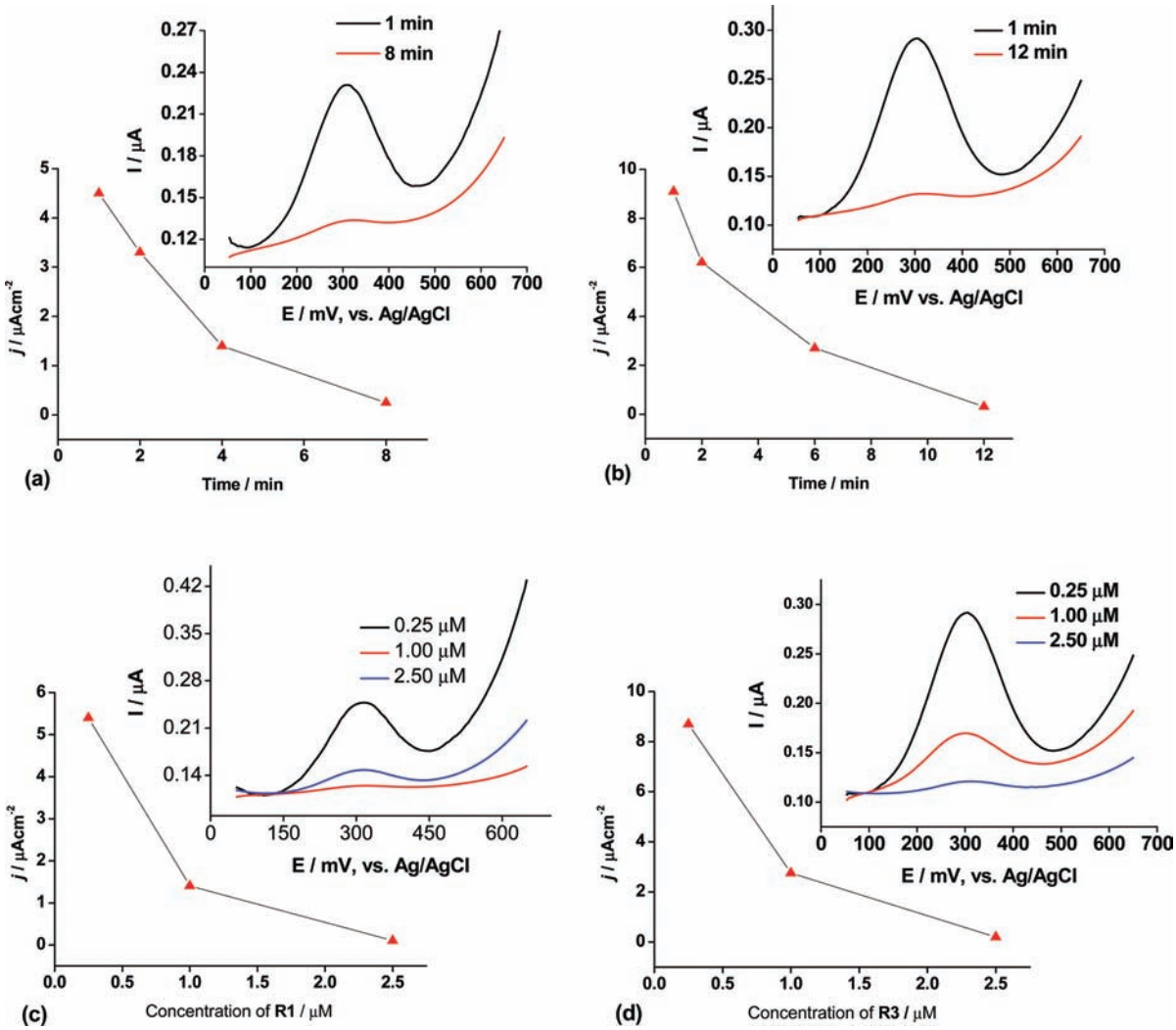

Figure 2. Dependence of the square-wave oxidation peak current density (j/μA cm^{-2}) on the incubation time (a, b) and concentration of **R1** and **R3** (c, d) for the detection of the 25 nM TP1 sequence at the Au/CP1/TP1/**R1** (a, c) and Au/CP1/TP1/**R3** electrodes (b, d) in tris-HCl buffer solution (pH 7.4). Insets show the square-wave voltammograms under designated conditions with a dc potential step of 4 mV, an amplitude of 50 mV, and a frequency of 25 Hz.

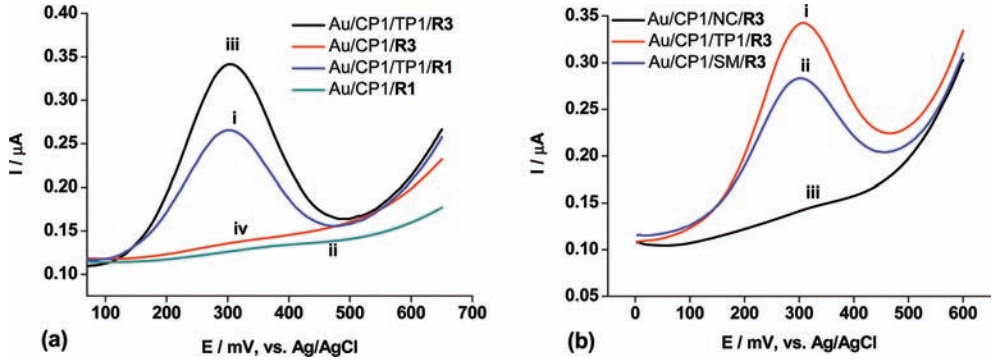

Figure 3. Square-wave voltmmograms obtained at (a) **R1**- and **R3**-functionalized electrodes before (ii, iv) and after (i, ii) hybridization with a 50 nM solution of the TP1 sequence. (b) **R3**-functionalized electrodes after hybridization with a 50 nM solution of the TP1 sequence (i) and either a 50 nM solution of single-base mismatched sequence (ii) or a 1.0 μM solution of noncomplementary (iii) sequence. Other experimental conditions are as in the caption to Figure 2.

Detection of Sequence-Selective Hybridization. Under optimized conditions, DNA-mediated charge transport can be used to detect the hybridization of the target DNA probe with the capture probe. Figure 3a illustrates the square-wave voltammetric responses at the Au/CP1/TP1/**R1** and Au/CP1/TP1/**R3** electrodes before (ii and iv) and after (i and iii) hybridization with the 50 nM target TP1 sequence. As shown in curves i and iii, the characteristic enhancement in current responses for the electrode after hybridization arises from favorable long-range charge transport through the duplex layer.[18–20] The thymines and TpT groups are located in the middle and proximal end with respect to the −SH group in the CP1 sequence. The attachment of **R1** and **R3** molecules at these positions results in long-range charge transport between the redox centers and

the electrode. The small current response detected with the highly sensitive square-wave method at the capture probe modified control Au/CP1/**R1** and Au/CP1/**R3** electrodes (curves ii and iv) also indicated a low level of charge transport between the redox center on ss-DNA and the electrode. As mentioned above, the CP1 sequence has thymines and TpT groups located in the middle and proximal end. The **R1** and **R3** configurations with the thymine bases located at the middle of the CP1 sequence could allow this low level of charge transport. It is also noted that the square-wave voltammetric peak currents obtained after 1 min incubation time at the Au/CP1/TP1/**R1** electrode are much smaller than those obtained at the Au/CP1/TP1/**R3** electrode. This also can be explained by taking into account the smaller binding constant for the **R3** molecules with the thymines and TpT groups in the duplex structure. It has previously been shown that the binding constant for **R3** is 300 times smaller than that for **R1**,[22] implying that **R3** is less effective for disrupting the base-pair stacking after 1 min of the incubation. Consequently, the Au/CP1/TP1/**R3** electrode allows better charge transfer through the duplex layer and, hence, offers higher sensitivity for DNA detection.

Square-wave voltammograms were recorded at the Au/CP1/TP1/**R2** (Figure S3, curves a and b, Supporting Information) and Au/CP1/TP1/**R4** electrodes (curves c and d) in 100 mM tris-HCl buffer under conditions given in the figure caption. The small oxidation peak observed at both the Au/CP1/TP1/**R2** and Au/CP1/TP1/**R4** electrodes in the presence of 500 nM TP1 target sequence is indicative of very weak binding of **R2** and **R4** molecules to the duplex layers, as outlined in Schemes S1 and S2 (Supporting Information). While both electrodes exhibit an oxidation peak, the relatively larger abundance of receptor **R4** molecules, arising from a larger number of active hydrogen bonding sites available in the duplex backbone, results in higher peak currents at the Au/CP1/TP1/**R4** electrode relative to that obtained at the Au/CP1/TP1/**R2** electrode. Importantly, under the optimized experimental conditions, the peak currents obtained for a 50 nM solution of TP1 at the Au/CP1/TP1/**R1** or Au/CP1/TP1/**R3** electrodes are much higher than those obtained at the Au/CP1/TP1/**R2** and Au/CP1/TP1/**R4** electrodes for a 500 nM concentration of TP1.

Concentration Dependence. The voltammetry at ferrocene bearing receptor-functionalized duplex sensing layers provides quantitative information related to the presence of the target DNA in the sensing layers. To test the sensitivity of the methods described in Scheme 1, detection of target ss-DNA (TP1) has been examined at concentrations ranging from 100 pM to 10 μM. The Au/CP1 electrodes were hybridized with different concentrations of the TP1 sequence followed by immobilization of 0.25 μM solutions of either **R1** or **R3**. The square-wave voltammograms obtained in 100 mM tris-HCl buffer (pH 7.4) with different concentrations of TP1 at the Au/CP1/TP1/**R1** and Au/CP1/TP1/**R3** electrodes are shown in Figures S4 and S5 (Supporting Information), respectively. For both electrodes, the peak current increased with concentration of the target sequence. This peak current enhancement is attributed to the increase in the association of the TP1 sequence, via the hybridization to the preimmobilized capture probe (CP1), which is responsible for an increase in the amount of **R1** or **R3** molecules in the duplex layer, and increases as the concentration of the target ss-DNA sequence (TP1) is increased. As detailed in Figures S4 and S5 (Supporting Information), target concentrations as low as 100 pM could be detected at both the Au/CP1/TP1/**R1** and Au/CP1/TP1/**R3** electrodes. When the target concentration was less than 100 pM, the signal was indistinguishable from the background and was comparable to the signal intensity of the control Au/CP1/**R1** or Au/CP1/**R3** electrodes (see curves ii and iv in Figure 3a). The effect of the binding of **R1** or **R3** to the Au/CP1/TP1 electrode on the current signal was reproducible, with a relative standard deviation (RSD) of 4.5−6.3% for four independently prepared electrodes.

Detection of Noncomplementary and Mismatched Sequences. To evaluate the discrimination of a noncomplementary DNA sequence, a duplex layer was fabricated using the large excess of the noncomplementary target sequence (NC, Table 1). The NC sequence was hybridized with the preimmobilized CP1 sequence onto the Au surfaces. After performing the hybridization step, the duplex layer was immersed in 100 mM tris-HCl containing 0.25 μM **R3** receptors for 1 min. Figure 3b (curve iii) shows the square-wave voltammetric responses for the 1.0 μM noncomplementary DNA sequence at the Au/CP1/NC/**R3** electrode. Clearly, the small current response obtained at the Au/CP1/NC/**R3** electrode is similar to that obtained at the control Au/CP1/**R3** electrode (curve iv in Figure 3a), indicating the binding of the noncomplementary DNA sequence to the capture probe immobilized surface to form the duplex layer, and hence, long-range charge transport through the duplex DNA is not significant.

The detection of mismatches was also investigated using a single-base (C−A) mismatched sequence (SM, Table 1). Figure 3b (curve ii) shows the square-wave voltammograms obtained at the Au/CP1/SM/**R3** modified electrodes in the presence of 50 nM SM sequence. These data clearly illustrate the usefulness of **R3** as a signaling compound to differentiate between a perfectly matched (curve i) and a single-base mismatched sequence (curve ii). Compared to the complementary target sequence (TP1), an approximate decrease in current of 30% was observed for the SM sequence at the Au/CP1/SM/**R3** electrode. We anticipated that the C−A mismatch in the SM sequence caused additional perturbation of the base-pair stacking, which decreased the long-range charge transport through the duplex layer, resulting in a decrease in current. The ability of **R3** to detect mismatches is consistent with the previous studies of DNA-mediated long-range charge transfer approaches for mismatch detection.[18,19]

Control Experiments. To gain a better understanding of the impact of the interaction of receptor **R1** and **R3** with the thymine (or TpT group) and phosphate moiety within the target sequence and, hence, the influence of these binding interactions on the Fc oxidation process at the receptor-functionalized duplex electrodes, a series of control experiments were conducted employing different target sequences with and without thymine bases (Table 1). In these DNA sequences, the A and T bases in the TP1 sequence were replaced with the C and G bases, respectively. Initially, a control experiment was conducted with the DNA sequences that was modified with the TpT group located at the proximal (hereafter referred to as TP2) and distal (hereafter referred to as TP3) end (with respect to the 3′-end) of the sequence. These two sequences, and their complementary capture sequences, were employed to fabricate the DNA duplex layers on the Au electrode. Chronocoulometric responses showed that the amount of ds-DNA immobilized on the electrode surface was identical in both cases. For the Au/CP2/TP2/**R3** and Au/CP3/TP3/**R3** electrodes, the analysis of 50 nM solutions of both the TP2 and TP3 sequences showed a lower response for the oxidation of surface-bound Fc (curves i and ii in Figure 4a), attributed to the lower abundance of the **R3**

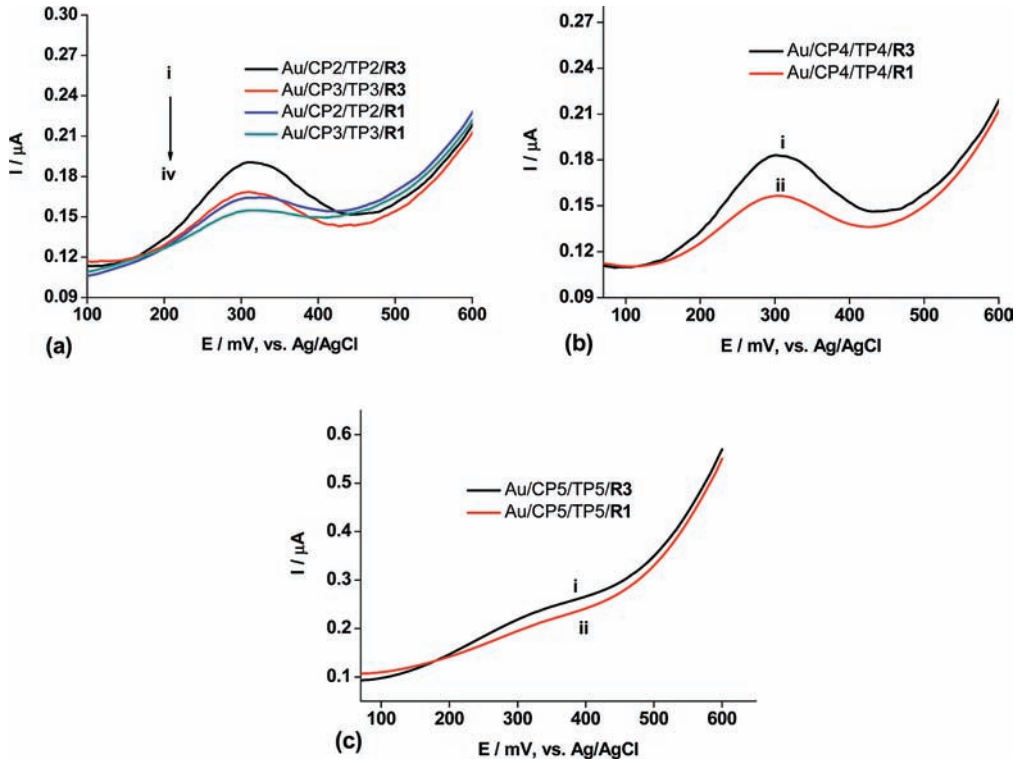

Figure 4. Square-wave voltammograms obtained at the **R1**- and **R3**-functionalized electrodes after hybridization to 50 nM solution of TP2 (i, iii in a), TP3 (ii, iv in a), TP4 (b), and TP5 (c) in 100 mM tris-HCl buffer solution. Other experimental conditions are as in the caption to Figure 2.

molecules on the duplex layers arising from a reduction in the TpT binding present in the TP2 and TP3 sequences. Since the binding between the TpT group and **R3** molecules could disrupt the A−T bonds at the proximal and distal end of the sensing layer in a similar fashion, one could expect an equal perturbation of the base-pair stacking for both the cases and hence equal voltammetric responses for both the Au/CP2/TP2/**R3** and Au/CP3/TP3/**R3** electrodes. However, when the TpT group is located at the distal end of the duplex DNA structure, a reduction in the oxidation currents of only 30% was observed at the Au/CP3/TP3/**R3** electrode (curve ii). These data clearly indicate that the DNA-mediated charge transport is much easier for the ds-DNA structure with the TpT groups located at the proximal end of the layer. A similar conclusion can be made for the data at the Au/CP2/TP2/**R1** and Au/CP3/TP3/**R1** electrodes (curves iii and iv in Figure 4a).

The target DNA sequence and corresponding complementary capture probe also were customized by replacing the A and T bases in the TP1 sequence with the C and G bases, except for the two thymine bases at the proximal end of the TP1 sequence (with respect to the 3′-end) (see TP4 and CP4, Table 1). Under the experimental conditions relevant to Figure 4a, the Au/CP4/TP4/**R3** (i) electrode provides a higher current than the Au/CP4/TP4/**R1** (ii) electrode in the presence of 50 nM TP4. In CP4/TP4 duplex electrodes, **R1** is proposed to bind as outlined in Scheme 2B and **R3** as in Scheme 2C. Since the binding constants for both are similar,[22] analogous attachment of Fc-bearing complexes and, hence, perturbation of the base-pair stacking for both the binding modes is expected, which should lead to similar electrochemical responses. However, the **R1** receptor binds to two thymines in the proximal end of the CP4/TP4 duplex, whereas **R3** binds to only one thymine unit. Consequently, a higher number of **R3** molecules will attach on the duplex layer, which may account for the higher current detected at the Au/CP4/TP4/**R3** electrode.

In another control experiment, the effect of the binding of **R1** and **R3** to the DNA sequence was examined without thymines or TpT groups in the complementary target and its capture probe (TP5 and CP5, Table 1). The Au/CP5/TP5/**R1** and Au/CP5/TP5/**R3** electrodes were fabricated employing the optimized binding conditions. Negligible square-wave voltammetric responses for oxidation of surface-bound Fc were observed for a 50 nM solution of TP5 at the Au/CP5/TP5/**R3** and Au/CP5/TP5/**R1** electrodes (curves i and ii in Figure 4c). These data imply that the association of **R1** and **R3** molecules on the CP5/TP5 duplex layer via the hydrogen bonding is not significant, under the experimental conditions employed.

Catalytic Enhancement of the Voltammetric Signal. Scheme 3 outlines the sensing protocol used to achieve signal amplification by electrocatalytic oxidation of diethylamine by the surface-bound Fc electrocatalyst. **R1**- or **R3**-functionalized duplex layers containing different concentrations of target sequence were fabricated following the method described in the Experimental Section. Modification of DNA duplex electrodes with **R1** or **R3** was achieved by incubation for 1 min in tris-HCl buffer solution containing 0.25 μM **R1** or **R3** receptors. Electrocatalytic experiments were undertaken by immersing the **R1**- or **R3**-functionalized duplex electrodes in a 100 mM tris-HCl buffer (pH 7.4) solution containing 2.5 mM diethylamine. It should be noted that under these solution conditions diethylamine is protonated (for simplicity, however, protonated diethylamine is referred to as DEA). Figure 5a shows the effect of the catalytic cycle on the cyclic voltammetric current response of DNA hybridization on the CP1/TP1/**R3** sensing layer. The irreversible oxidation peak at 440 mV seen in Figure 5a (curve iii) results from the electrocatalytic oxidation of DEA by the surface-bound

Scheme 3. Schematic Representation of the Electrocatalytic Oxidation of Diethylamine by the Fc Bearing Cyclen Complex at a DNA-Modified Gold Electrode[a]

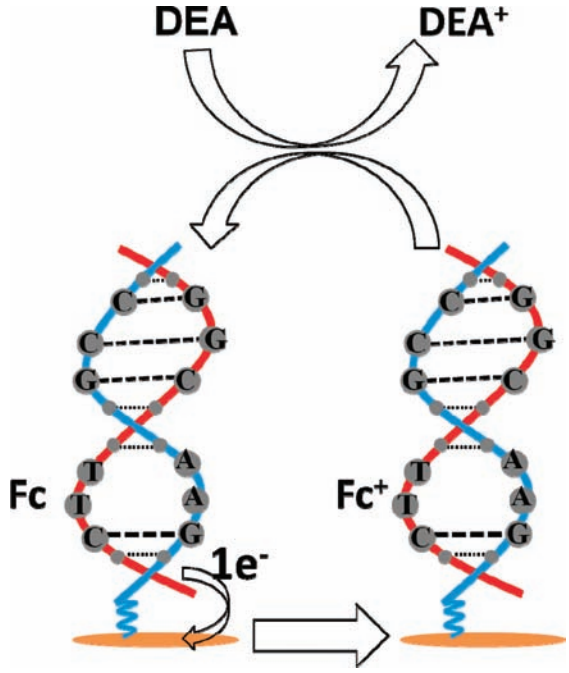

[a] In practice DEA^+ is unstable in aqueous solutions.

$Fc^{0/+}$ process. Importantly, the magnitude of the catalytic peak current indirectly reflects the concentration of TP1 (50 nM) anchored to the duplex sensing layer. The catalytic response obtained at the Au/CP1/**R3** electrode with no target sequence present (curve i) was also examined. It is evident that electrocatalysis on the Au/CP1/**R3** electrode results in a response similar to that obtained at the Au/CP1/**R3** electrode, with no catalytic step (curve iii in Figure 1a). This is attributed to unfavorable charge transport through the CP1/**R3** layer as described above. A similar catalytic feature for the detection of DNA hybridization, but with lower sensitivity, was attained at the Au/CP1/TP1/**R1** electrode (not shown).

The addition of diethylamine to the electrolyte produces dramatic changes in the cyclic voltammograms of **R3**, with an obvious increase in oxidation peak currents and a concomitant decrease in reduction peak currents. This catalytic mechanism has been described previously by Nicholson and Shain[29] for the general case in which the electrode process consists of a reversible charge transfer followed by the chemical regeneration of the reduced species (Scheme 3). The oxidation reaction is thermodynamically favorable because the surface-bound Fc^+ is capable of oxidizing solution-phase DEA. The reverse reaction, however, does not occur because it requires the thermodynamically unfavorable electron transfer from Fc to DEA^+. The absence of a reduction peak for DEA^+ and the positive shift of the oxidation peak for the DEA strongly suggest that DEA oxidation is occurring via the proposed redox reaction involving Fc. This electrocatalytic reaction is expected to allow DNA hybridization detection at the femtomolar level.

The effect of DEA concentration on the electrocatalytic current obtained by dc cyclic voltammetry at the Au/CP1/TP1/**R3** electrode was examined. The peak current was found to increase with concentration of DEA but leveled off when the concentration of DEA was above 2.5 mM (Figure S6a, Supporting Information). Thus, 2.5 mM DEA was selected for catalytic experiments described below with the Fc-bound duplex electrodes.

Analytical Performance Achieved by Employing the Electrocatalytic Reaction between the Surface-Bound $Fc^{0/+}$ Process and DEA. (i) Effect of Target Concentration. Figure 5b shows the dependence of the electrocatalytic oxidation current density derived from Au/CP1/TP1/**R3** electrodes on the concentration of the target DNA solutions over the concentration range of 150 fM to 10 μM. Under conditions of cyclic voltammetry, detection over a wide dynamic range (150 fM and 1.0 μM) covering 6 orders of magnitude of concentration was observed. The detection limit for the target DNA was estimated to be 100 fM based on S/N = 3, which is 10-fold lower than that reported previously in enzyme-free methods.[30,14e] The detection limit for the **R1**-functionalized Au/CP1/TP1 duplex electrode was 250 fM. These detection limits are similar to the lowest values obtained in bioassays based on carbon nanotube-derived amplification,[17] enzyme-amplified amperometric detection with a microelectrode,[31a] and DNA hybridization using biometallization.[31b] The detection limit is coupled with excellent reproducibility. Two series of six repeat measurements for a 150 pM TP1 target DNA concentration each yielded RSD values of 8.2% (n = 6).

(ii) Detection of Noncomplementary and Mismatched Sequences. Figure 6a shows differences found in detection of complementary (TP1) and noncomplementary target DNA (NC). At the Au/CP1/TP1/**R3** and Au/CP1/TP1/**R1** modified electrode, a sharp increase in the oxidation peak currents for 50 nM TP1 was observed after introduction of the catalytic step (curves i and ii in Figure 6a). However, when NC was used, the peak current at the Au/CP1/NC/**R3** and Au/CP1/NC/**R1** electrodes (curves iii and iv) was similar to that obtained at the control Au/CP1/**R3** electrode (e.g., before hybridization) (curve i in Figure 5a). These results indicate that the long-range charge transfer through the Au/CP1/NC duplex layer, as explained above, is not significant. Moreover, nonspecific adsorption of the NC sequence onto the Au/CP1 layer, and hence the attachment of the **R1** or **R3** to the NC-attached duplex layer, did not occur.

Figure 6b compares the catalytic responses obtained for the target (Au/CP1/TP1/**R3**) and single-base mismatched (Au/CP1/SM/**R3**)-modified electrodes. The C−A mismatch in the SM sequence result in a >25% decrease in oxidation peak, indicating stronger perturbation of charge transport from the Fc center to the electrode surface through the duplex layer. Importantly, the peak currents obtained at the Au/CP1/SM/**R3** electrode, after employing the catalytic step, are much higher than those obtained before employing the catalytic step. As a consequence of the catalytic reaction, there is a significant improvement in selectivity for detecting the single-base mismatched sequence by the coupling of the electrocatalytic reaction step at the DNA-mediated electrode. The ability to differentiate between a complementary sequence and a single-base mismatched (or noncomplementary) sequence also was achieved by Barton et al.[19] in which methylene blue coupled to $[Fe(CN)_6]^{3-}$ was used to detect mutations by electrocatalysis at DNA-mediated electrodes.

(29) Nicholson, R. S.; Shain, I. *Anal. Chem.* **1964**, *36*, 706.
(30) (a) Polsky, R.; Gill, R.; Kaganovsky, L.; Willner, I. *Anal. Chem.* **2006**, *78*, 2268. (b) Lieber, C. M.; Hahm, J. *Nano Lett.* **2004**, *4*, 51. (c) Wang, J.; Liu, G.; Merkoci, A. *J. Am. Chem. Soc.* **2003**, *125*, 3214.
(31) (a) Zhang, Y.; Kim, H.; Heller, A. *Anal. Chem.* **2003**, *75*, 3267. (b) Hwang, S.; Kim, E.; Kwak, J. *Anal. Chem.* **2005**, *77*, 579.

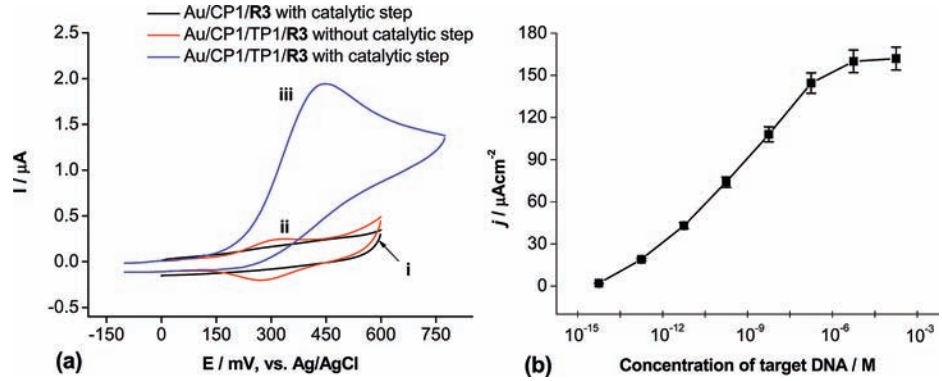

Figure 5. (a) Cyclic voltammograms obtained at a scan rate of 100 mVs^{-1} at the Au/CP1/TP1/**R3** electrode for a 50 nM solution of TP1 target sequence with 2.5 mM DEA (iii) and without DEA (ii) in tris-HCl buffer solution. Curve (i) shows the control voltammogram obtained for the Au/CP1/**R3** electrode. (b) Dependence of the oxidation current density on the TP1 concentration at the Au/CP1/TP1/**R3** electrode.

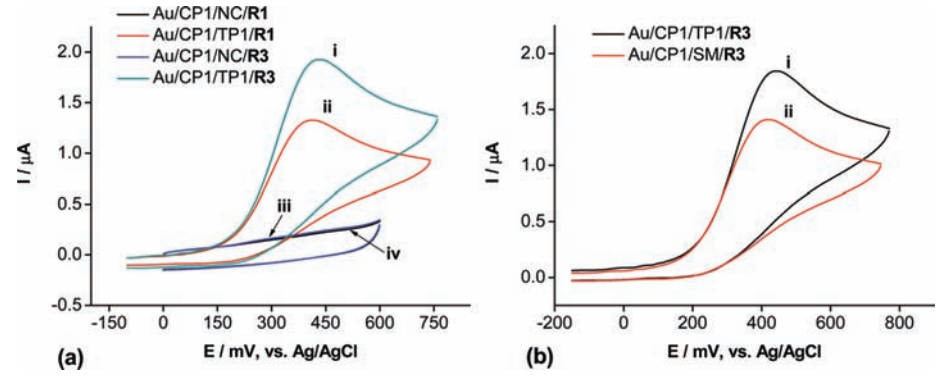

Figure 6. Cyclic voltammograms obtained at (a) **R1**- and **R3**-functionalized electrodes after hybridization to (a) 50 nM solutions containing the target TP1 (i and ii) and noncomplementary (iii, iv) sequences. (b) An **R3**-functionalized electrode after hybridization to a 50 nM solution of either the target TP1 (i) or the single-base mismatched (ii) DNA sequence. Other experimental conditions are as in the caption to Figure 5.

Long-Term Stability. The long-term stability of the biosensing layer was examined by measuring the electrochemical response of an **R3**-functionalized duplex electrode for 20 days, storing the electrode in 100 mM tris-HCl buffer solution (pH 7.4) at 4 °C. After 20 days, the oxidation peak current density decreased by only 9.3% for the 150 pM target TP1 sequence (Figure S6b, Supporting Information). The gradual decrease is likely to be a result of the slow deactivation of the **R3**-functionalized sensing layers that takes place when experiments are repeated with the same electrode.

Conclusions

A selective, sensitive, and simple electrochemical assay based on DNA-mediated charge transport coupled to a catalytic reaction between surface-bound ferrocene moieties and diethylamine present in solution has been developed. **R1** and **R3** receptor molecules form a very strong and selective chelate complex by interacting with the T bases or TpT groups in the duplex DNA structure at neutral pH. No oxidation current is observed prior to the complexation of the **R1** and **R3** with the target sequence to form the duplex structure on the Au electrode. Upon complexation, an electrochemical response arising from the oxidation and reduction of the surface-bound Fc following duplex formation is observed which decreases with time. The suppression of the current is hypothesized to be a consequence of the disruption of the hydrogen bonding between A−T base pairs in the duplex layer, which makes long-range charge transport more difficult. Using optimized time and ionic strengths for the incubation of the duplex sensing layer in the receptor solutions, the DNA biosensor can discriminate between the complementary and either single-base pair mismatched or nonomplementary DNA sequences.

A significant enhancement in current signal was achieved by introducing an electrocatalytic step, which involved the addition of 2.5 mM DEA into the 100 mM tris-HCl buffer solution used for the electrochemical measurements with the **R1**- or **R3**-immobilized duplex sensing layers (pH 7.4). Electrocatalysis enabled the selective detection of complementary over noncomplementary and single-base pair mismatched DNA sequences. Furthermore, a wide dynamic range of concentrations (150 fM to 1.0 μM) can be measured in a single assay format with a detection limit of 100 fM. The combination of simple fabrication and detection procedures as well as excellent stability and reproducibility implies that the sensor is a viable alternative to conventional enzyme- or nanocatalyst-based electrochemical detection methods. Since the method employs electrochemical detection, the design of an integrated, portable, and low-cost device for DNA detection should be achievable.

Acknowledgment. This work was supported by the Australian Research Council through the Federation Fellowship Scheme (AMB) and Australian Centre of Excellence for Electromaterials Science (LS).

Supporting Information Available: Schematic representations of the binding of **R2** and **R4** to the DNA duplex layers, chronocoulometric response curves of the duplex-modified electrode in the absence and presence of $[Ru(NH_3)_6]^{3+}$, the effect of incubation time and concentration of the **R2** and **R4** on the

oxidation current density obtained at Au/CP1/TP1/**R2** and Au/CP1/TP1/**R4** electrodes, square-wave voltammograms obtained at **R2**- and **R4**-functionalized electrodes before and after hybridization to the TP1 sequence, dependence of the oxidative voltammograms on the concentration of the TP1 sequence at the **R1**- and **R3**-functionalized electrode, dependence of the electrocatalytic current density on the concentration of DEA, and electrocatalytic current density as a function of storage time. This material is available free of charge via the Internet at http://pubs.acs.org.

JA1021365